# Supporting Information

## Strongly Photoluminescent and Radioluminescent Copper(I) Iodide Hybrid Materials Made of Coordinated Ionic Chains

Jingwen Chen, [a, b] Kang Zhou, [b] Jingbai Li, [b] Guozhong Xu, *[a] Xiuze Hei, *[b] Jing Li*[c, b]

[a] *College of Chemical Engineering, University of Science and Technology Liaoning, Anshan 114051, China.*

[b] *Hoffman Institute of Advanced Materials, Shenzhen Polytechnic University, 7098 Liuxian Blvd., Shenzhen, 518055 China.*

[c] *Department of Chemistry and Chemical Biology, Rutgers University, 123 Bevier Road, Piscataway, NJ 08854, USA.*

*E-mail: gz_xu@ustl.edu.cn; xiuzehei@szpu.edu.cn; jingli@rutgers.edu.*

**TABLE OF CONTENTS**

# S1. Methods

**Materials.** 1H-benzo[1,2,3]-triazole (99%); 1-bromo-2-chloroethane (98%); 1-bromo-3-chloropropane (98%); 3-Quinuclidinol (95%); Potassium iodide (99%); Potassium carbonate (99%); Acetone (99.5%); Acetonitrile (99.5%); Ethyl ether (99%); Copper iodide (98%). All materials are purchased from vendors and used directly without further purifications. 1-(2-chloroethyl)-1H-benzo[d][1,2,3]triazole (*Cl-ebt*) and 1-(3-chloropropyl)- 1H-benzo[d][1,2,3]triazole (*Cl-pbt*) were synthesized according to previously reported procedures.[1, 2]

**Preparation of $L_1$ I.**

*Cl-ebt* (0.9 g, 5 mmol) and KI (1.6 g, 10 mmol) were added with 30 ml acetone and stirred for 5 h at room temperature before drying under reduced pressure. The solid residue was wash with EtOAc, filtered to get filtrate. After removal of the solvent under reduced pressure, MeCN (50 ml) and 3-Quinuclidinol (0.64 g, 5 mmol) were added and stirring under 60 °C for 2 days. The reaction mixture was evaporated under reduced pressure, washed with ethyl ether and dried under vacuum. Recyclizing with EtOH gives the final product as white solid. The yield is 57%.

**Preparation of $L_2$ I.** $L_2$ I was prepared with a similar procedure as $L_1$ I but using *Cl-pbt*. White solid was obtained as final product. The yield is 63%.

**Synthesis of compound 1.** CuI (30 mg, 0.15 mmol) was first dissolved in KI saturated solution (1 ml) in a reaction vial. MeCN (1 ml) was added slowly as another layer, followed by the slow addition of $L_1$ I (40 mg, 0.1 mmol) EtOH solution (1 ml). The reaction was kept undisturbed at RT for 2 days to yield plate-like orange crystals. The yield is 46%.

**Synthesis of compound 2.** CuI (38 mg, 0.2 mmol) was first dissolved in KI saturated solution (1 ml) in a reaction vial. MeCN (1 ml) was added slowly as another layer, followed by the slow addition of $L_1$ I (42 mg, 0.1 mmol) MeOH solution (1 ml). The reaction was kept undisturbed at RT for 2 days to yield plate-like yellow crystals. The yield is 62%.

**Synthesis of compound 3.** Compound **3** was synthesized in the same way as that of compound **1**, using $L_2$ I as ligand. Needle-like orange crystals were obtained. The yield is 55%.

**Synthesis of compound 4.** Compound **4** was synthesized in the same way as that of compound **2**, using $L_2$ I as ligand. Plate-like yellow crystals were obtained. The yield is 44%.

**Characterizations.** Nuclear magnetic resonance (NMR) data was recorded using 400 MHz JEOL JNM-ECZ400S. Single crystal X-ray diffraction data were collected on a Bruker D8 Venture diffractometer. The structures were solved by direct methods and refined by full-matrix least-squares on $F^2$ using the Bruker SHELXTL package. The structures were deposited in Cambridge Crystallographic Data Center (CCDC) with numbers 2374849-2374852. Powder X-ray diffraction (PXRD) patterns were measured using Bruker D8 Advance X-ray diffractometer with Cu Kα radiation. Thermogravimetric analysis (TGA) were performed using the TA Instrument Q5000IR thermogravimetric analyzer. Optical absorption spectra were measured at room temperature on a Shimadzu UV-3600 UV–vis–NIR spectrometer. Photoluminescence quantum yields (PLQYs) were recorded using a C9920-02 absolute quantum yield measurement system (Hamamatsu Photonics). PL measurements were carried out on FLS1000 spectrofluorometer (Edinburgh Instruments). RL measurements were carried out on OmniFluo960-XrayP spectrofluorometer (Zolix Instruments). DFT calculations were carried out using VASP.

**Equations.**

The X-ray attenuation coefficient μ of a scintillator can be estimated using eq. S1[3]:

$$\mu = \frac{\rho Z^4}{AE^3} \qquad eq.S1$$

Where $\rho$ is the density, $Z$ is the atomic number, $A$ is atomic mass and $E$ is the incident X-ray energy. For a specific compound, instead of $Z$, the effective atomic number ($Z_{eff}$) is often used and be calculated from eq. 2[4]:

$$Z_{eff} = \sqrt[4]{\sum_i w_i Z_i^4} \qquad eq.S2$$

Where $w_i$ is the weight ratio of the $i$-th element of the material, $Z_i$ is the atomic number of the $i$-th element.

The emission intensity of a scintillator under X-ray irradiation can be calculated as following eq. 3[4]:

$$I = \frac{E}{\beta E_g} \times S \times Q \qquad eq.S3$$

Where $E$ is the energy of the incident X-rays, $\beta$ is a constant parameter, $E_g$ is the band gap of the materials, $S$ is the energy migration efficiency, and $Q$ is the quantum efficiency, which is equivalent in value to the PLQY.

Tetrahedral parameters of Δd (bond distance deviation) and Δθ (bond angle deviations) were calculated with the following equations[5]:

$$\Delta d = \frac{1}{4}\sum_{n=1}^{4}\left(\frac{d_n - d}{d}\right)^2 \qquad eq.S4$$

$$\Delta \theta = \frac{1}{6}\sum_{n=1}^{6}\left(\frac{\theta_n - \theta}{\theta}\right)^2 \qquad eq.S5$$

Where $d_n$ and $d$ are the individual bond distance and average bond distance within the tetrahedral, respectively. The $\theta_n$ and $\theta$ are the individual and average I-Cu-I / I-Cu-N bond angle in the tetrahedral.

## S2. $^{1}$H NMR spectroscopy.

All the $^{1}$H NMR spectra were collected using dimethyl sulfoxide-d6 as solvent. The peaks at 2.50 ppm and ~3.3 ppm are the residue DMSO and water peaks, respectively.

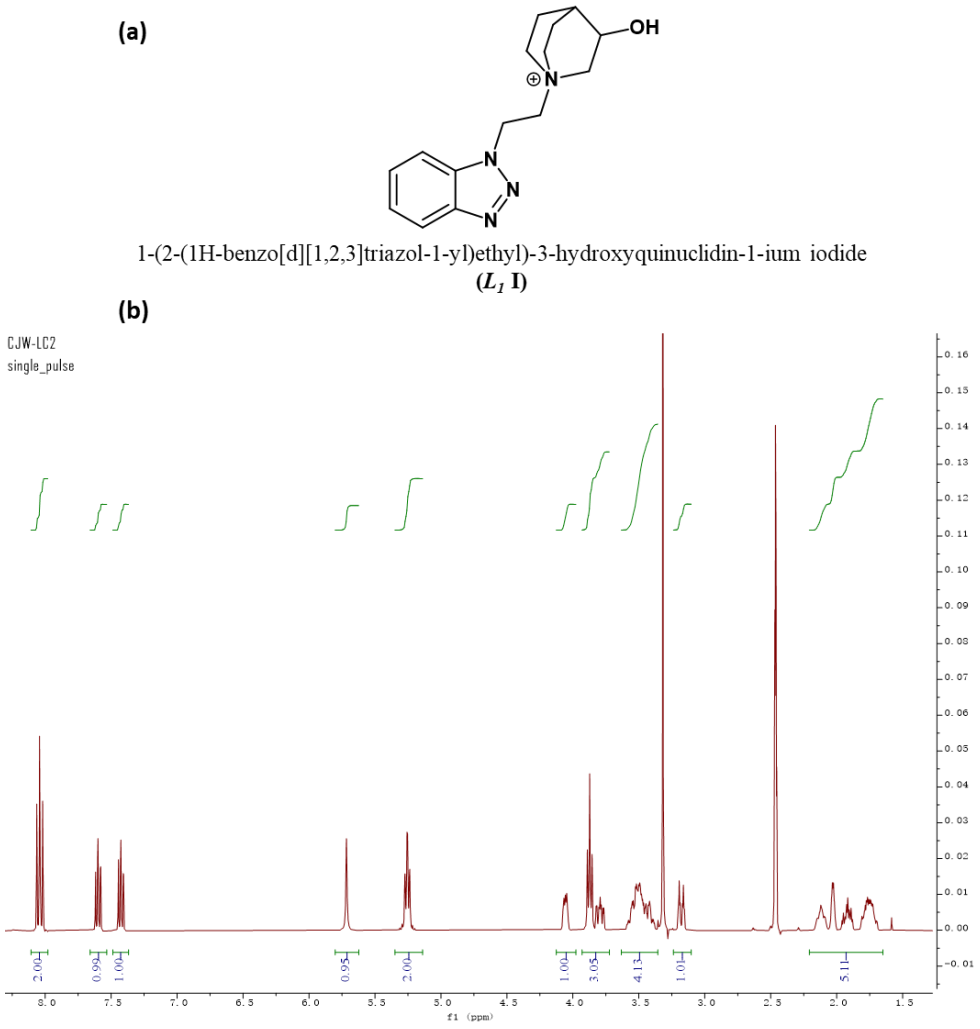


**Figure S1**. (a) Structural plot and (b) $^{1}$H NMR spectrum of $L_1$ I.

(a)

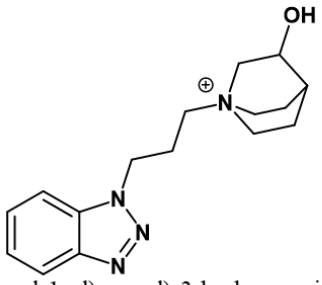


1-(3-(1H-benzo[d][1,2,3]triazol-1-yl)propyl)-3-hydroxyquinuclidin-1-ium iodide

(***L*** $_2$ **I)**

(b)

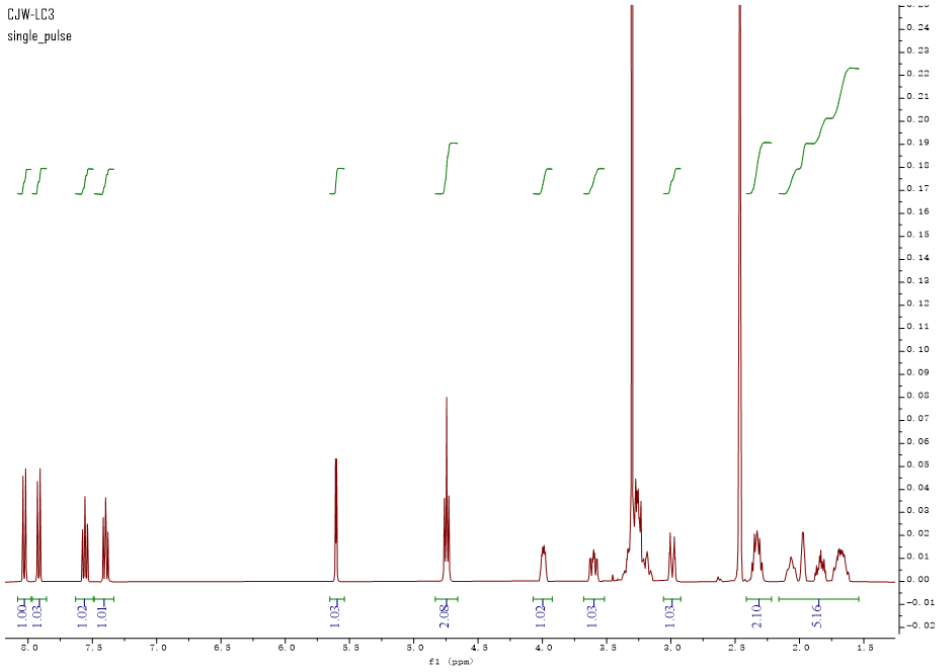


**Figure S2**. (a) Structural plot and (b) $^{1}$H NMR spectrum of $L_2$ I.

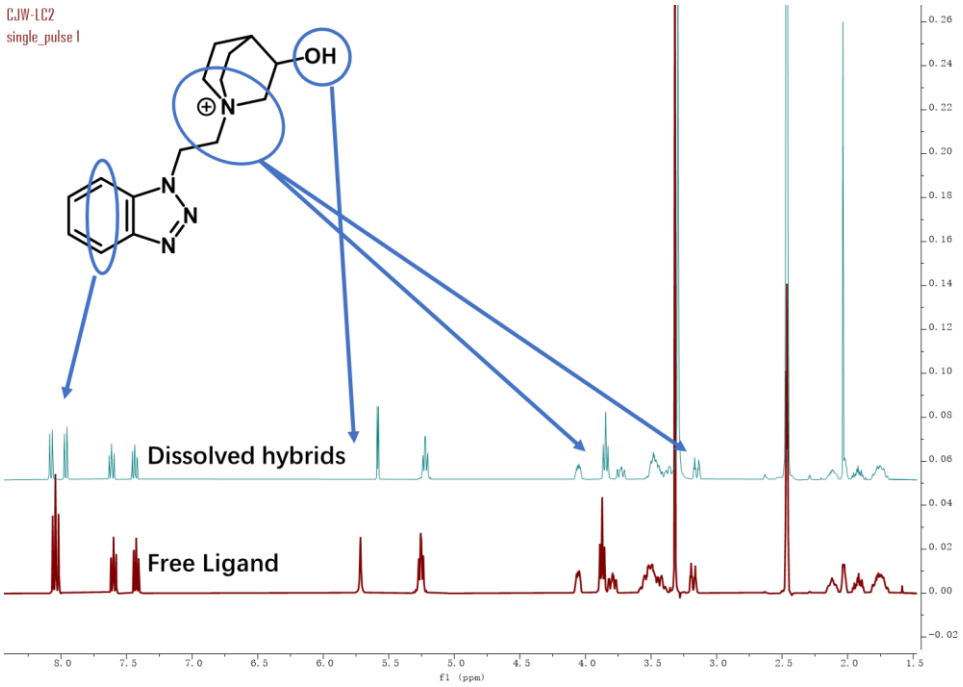


**Figure S3**. $^{1}$H NMR spectra of dissolved compound **1** (top) and free ligand $L_1$ I (bottom).

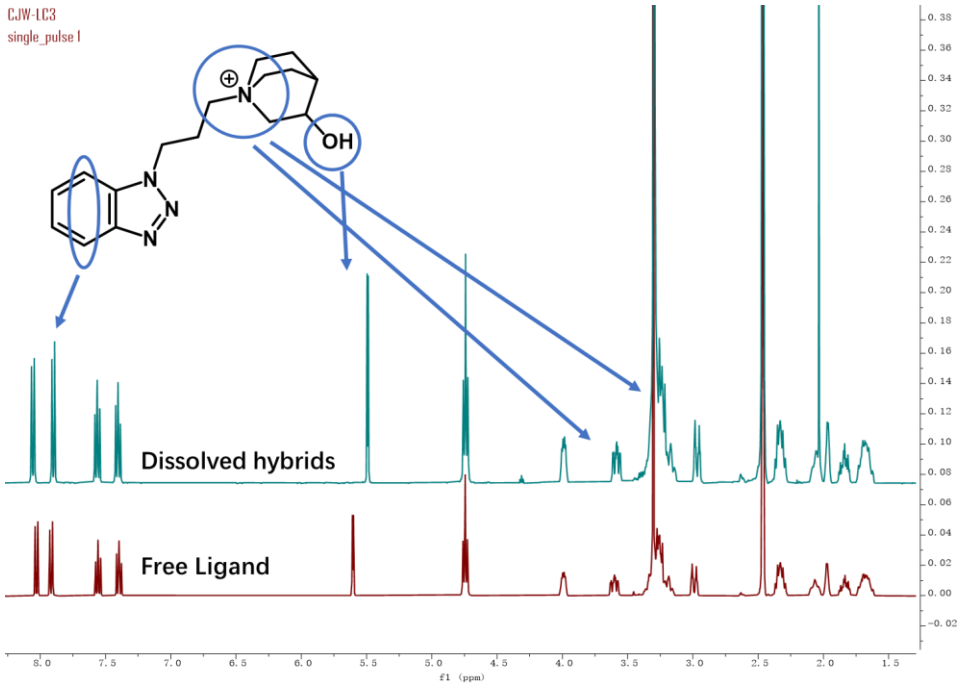


**Figure S4**. $^{1}$H NMR spectra of dissolved compound **3** (top) and free ligand $L_2$ I (bottom).

## S3. Crystal data and structural plots of compounds 1-4.

**Table. S1** Summary of crystallographic data of compounds **1-4**.

| **Compound** | **1** | **2** | **3** | **4** |
|---|---|---|---|---|
| Crystal System | monoclinic | monoclinic | monoclinic | triclinic |
| Empirical Formula | $C_{17}H_{24}Cu_2I_3N_5O$ | $C_{15}H_{19}Cu_2I_3N_4O_2$ | $C_{18}H_{26}Cu_2I_3N_5O$ | $C_{34}H_{47}Cu_4I_6N_9O_2$ |
| FW | 822.19 | 795.12 | 836.22 | 1629.36 |
| Space Group | $P2_1/c$ | $P2_1/n$ | $P2_1/c$ | $P$-1 |
| *a* (Å) | 10.8995(5) | 11.4886(10) | 11.4530(13) | 10.1107(15) |
| *b* (Å) | 16.7093(8) | 13.4361(10) | 17.025(2) | 11.2297(18) |
| *c* (Å) | 13.8142(6) | 15.0603(12) | 12.8883(13) | 11.9172(17) |
| α (°) | 90 | 90 | 90 | 73.930(6) |
| β (°) | 108.662(2) | 98.972(3) | 94.855(3) | 67.168(5) |
| γ(°) | 90 | 90 | 90 | 71.862(6) |
| V ($Å^3$) | 2383.60(19) | 2296.3(3) | 2504.1(5) | 1166.1(3) |
| Z | 4 | 4 | 4 | 1 |
| T (K) | 200.0 | 200.0 | 200.0 | 200.0 |
| λ(Å) | 0.71073 | 0.71073 | 0.71073 | 0.71073 |
| $R_1$ | 0.0540( 5231) | 0.0507( 4048) | 0.0605( 4436) | 0.0436( 4857) |
| $wR_2$ | 0.1117( 6693) | 0.1352( 5283) | 0.1352( 5854) | 0.1023( 5799) |

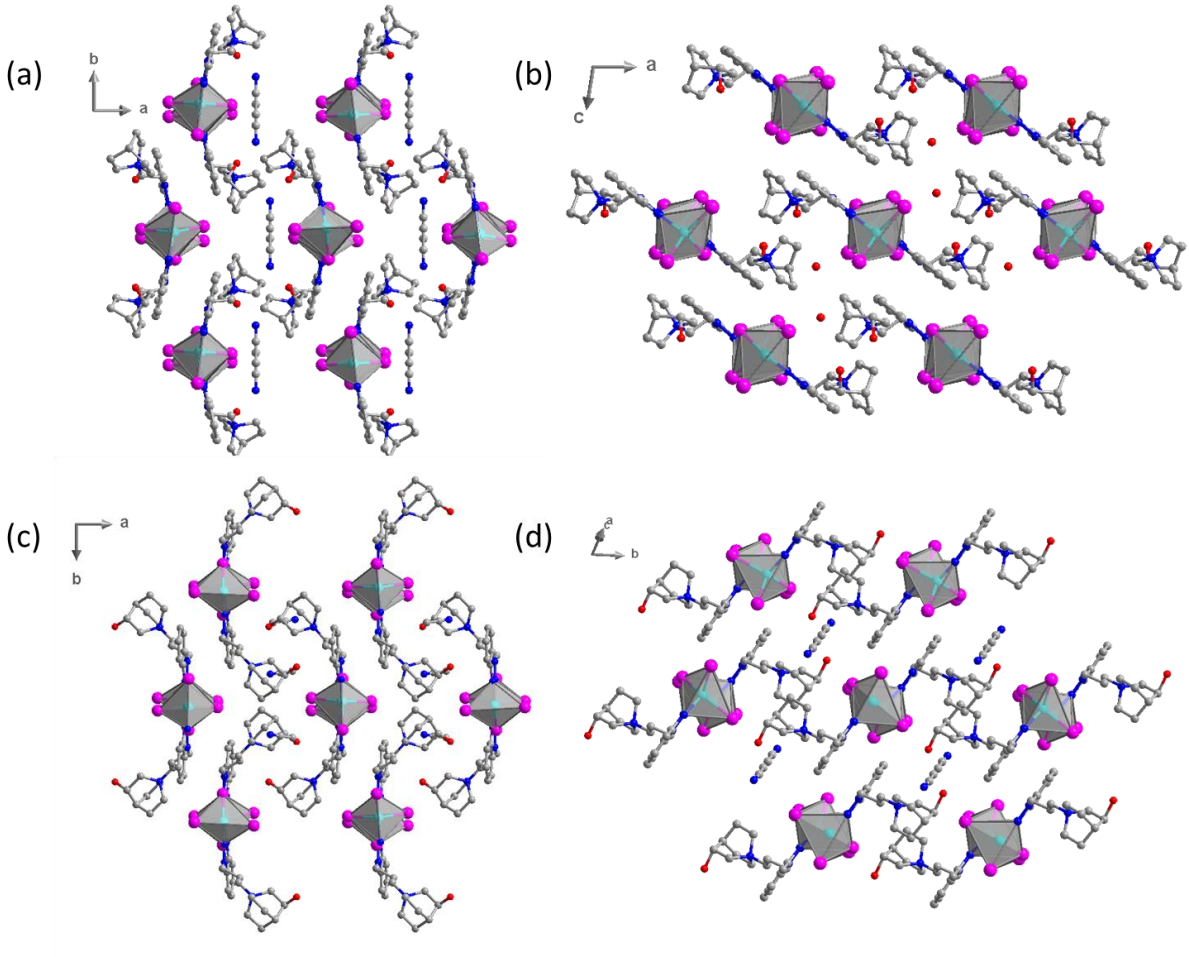


**Figure S5**. Structure plots of compounds (a) **1**, (b) **2**, (c) **3,** and (d) **4**. H atoms and disorders are omitted for clarity. Color scheme: cyan: Cu; purple: I; gray: C; blue: N; red: O.

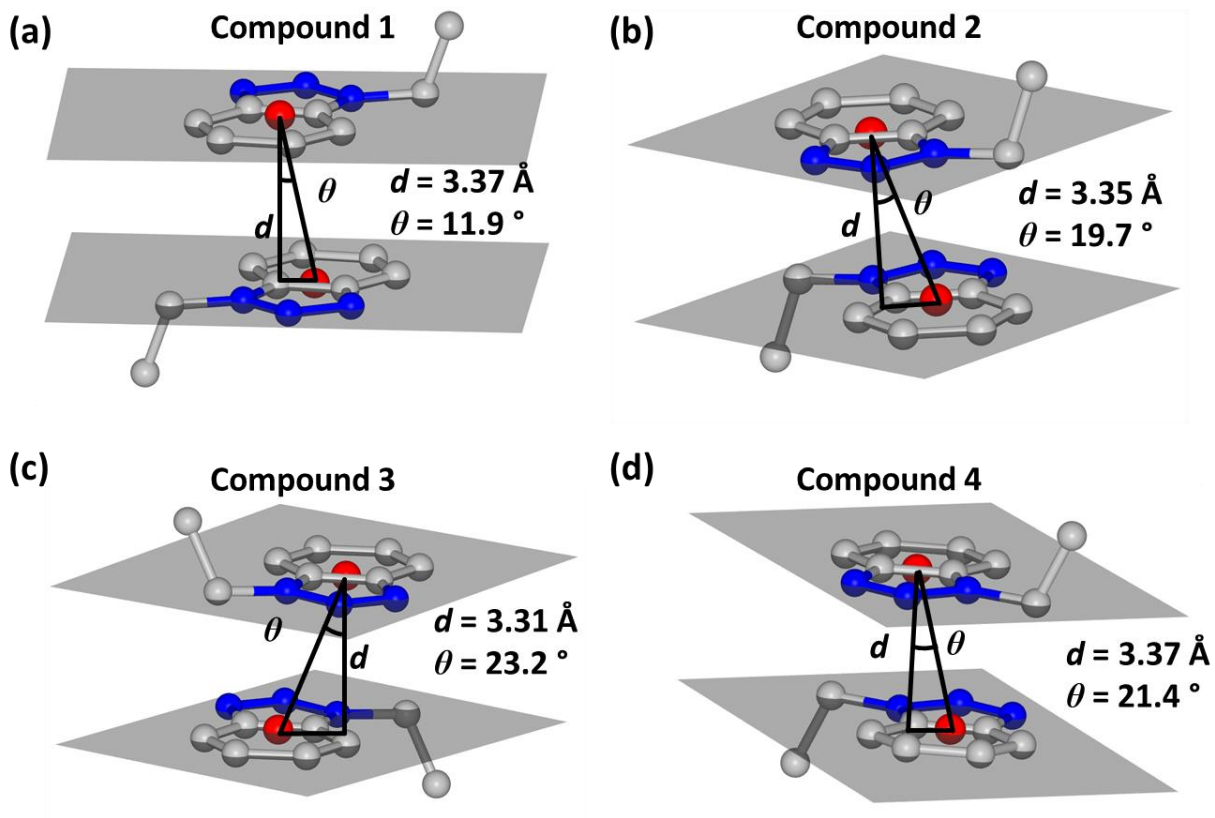


**Figure S6**. Close π–π interactions in all compounds. The two π systems are from two adjacent AIO chains. Color scheme: gray: C; blue: N; red: centroid. *d*: vertical distance between the adjacent π planes; *θ*: displacement angle, the angle between the centroid–centroid line and the vertical line.

## S3. DFT calculation results.

The geometry optimizations and electronic structure calculations for all compounds used the VASP 5.0.4 with a plane wave (PW) basis set and projected augmented wave (PAW) pseudopotentials (PPs). We employed the PBE flavor of the GGA PPs, and long-range dispersion interactions were considered by the DFTD3 scheme. The kinetic energy cut-off is 500 eV for the expansion of the wavefunctions. The convergence thresholds were set to $10^{-6}$ eV for energy and 0.05 eV/ Å for the norm of the atomic forces. The k-points in all calculations used for compounds **1**–**4** are 3×3×2, 3×3×2, 3×2×3, and 3×3×3 using the Gamma-centered mesh.

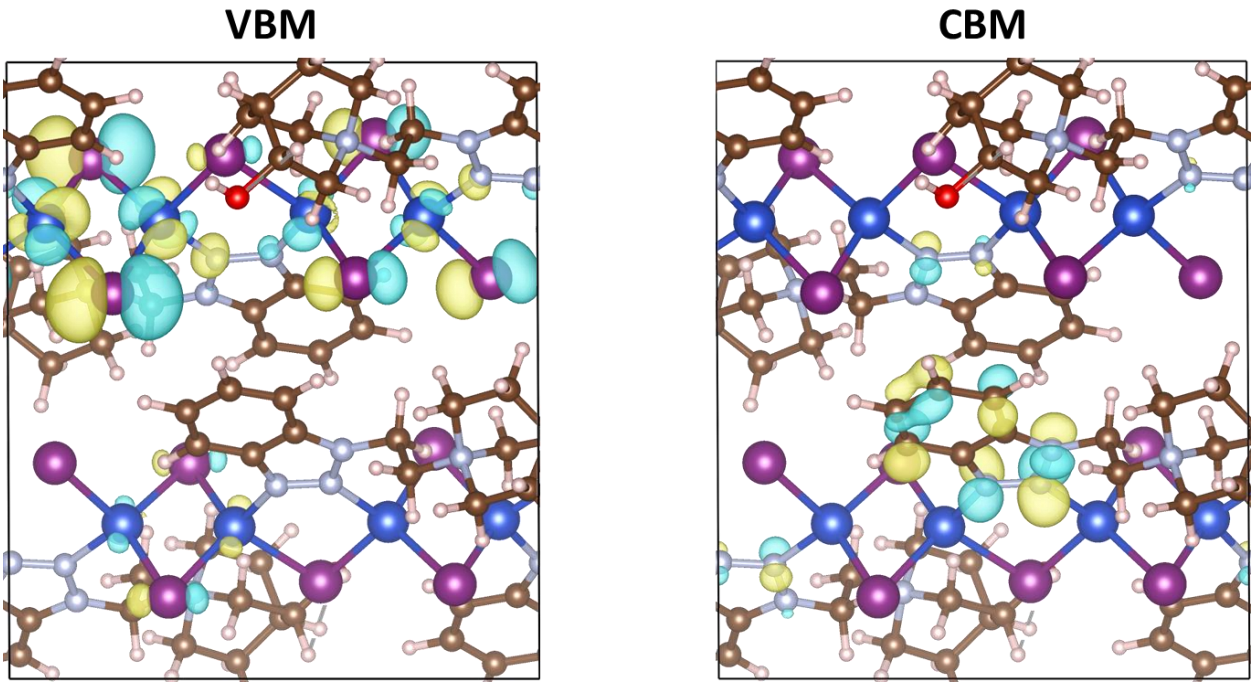


**Figure S7**. Computed wave functions of the VBM (left) and CBM (right) of compound **2**.

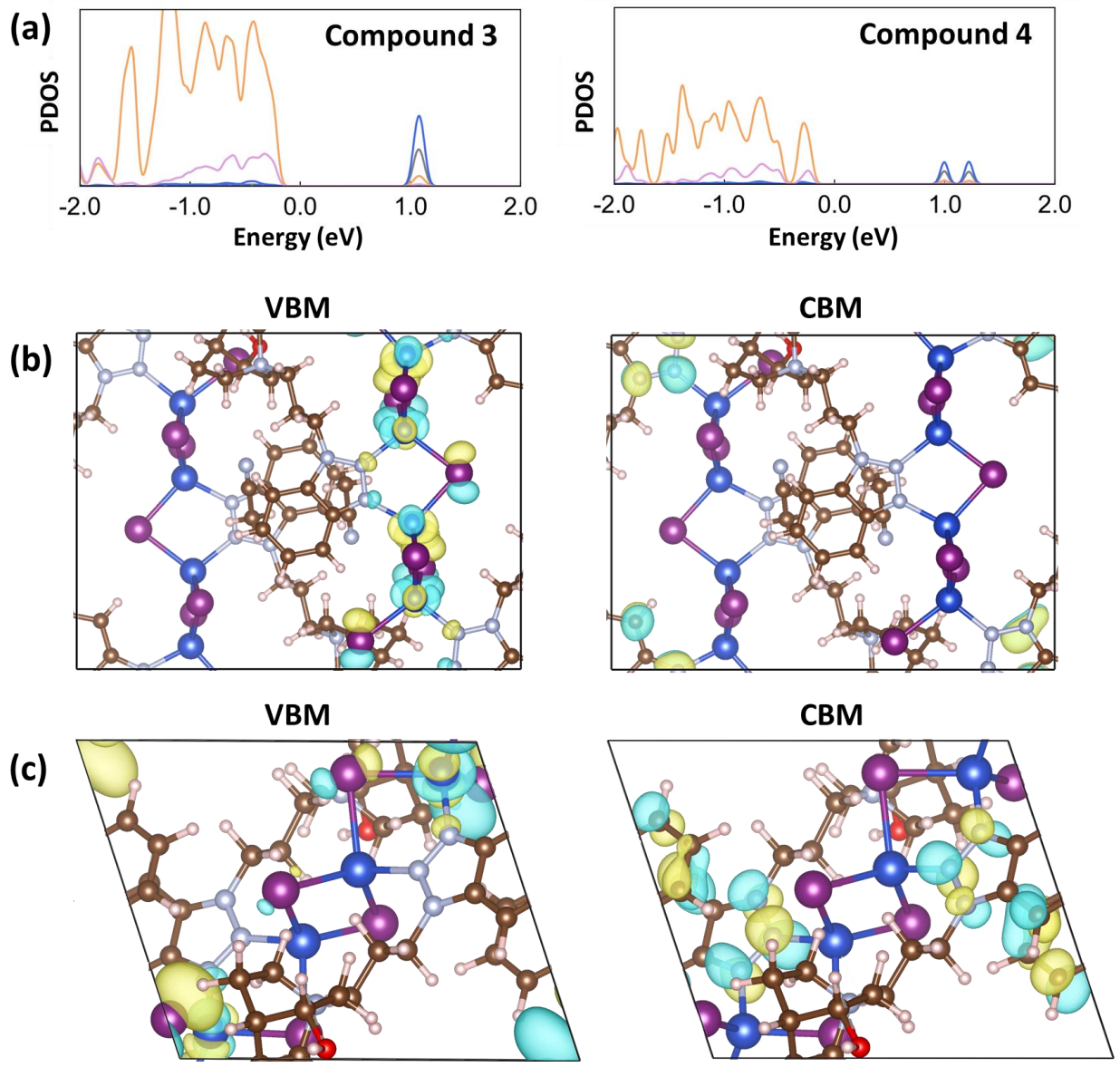


**Figure S8**. (a) Calculated projected density of states (PDOS) of compounds **3** and **4**. Color scheme: yellow: Cu 3d; purple: I 5p; blue: N 2p; black: C 2p. Computed wave functions of the VBM (left) and CBM (right) of compounds (b) **3** and (c) **4**.

# S4. Photophysical properties.

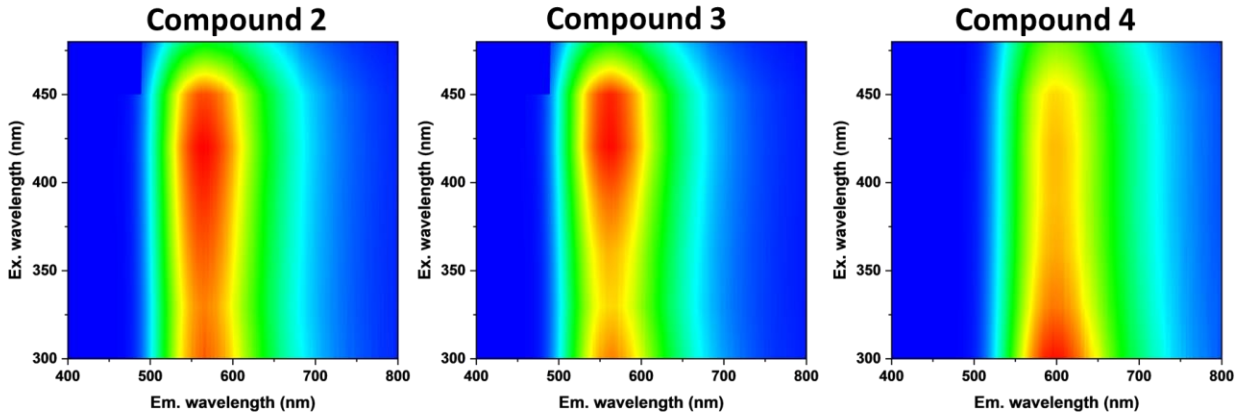


**Figure S9**. Excitation-dependent PL spectra of compounds **2-4.**

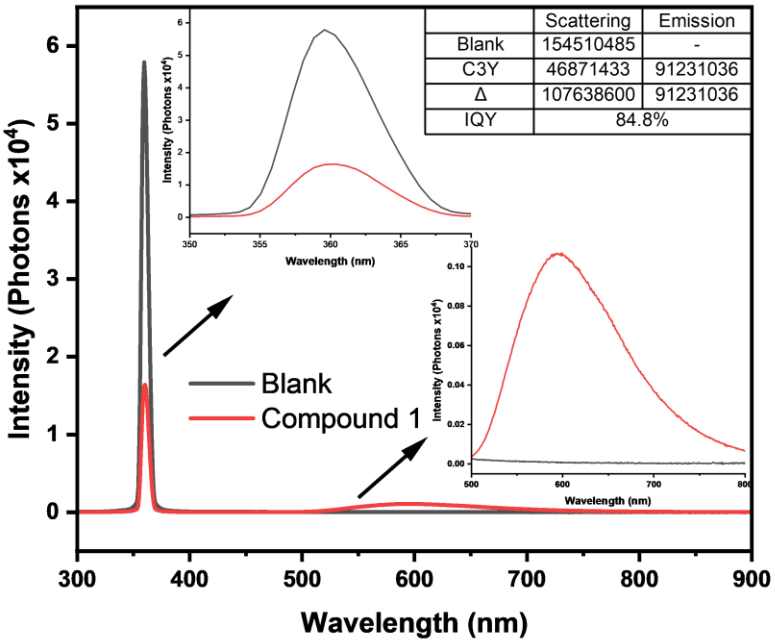


**Figure S10**. Details of PLQY measurement of compound **1.**

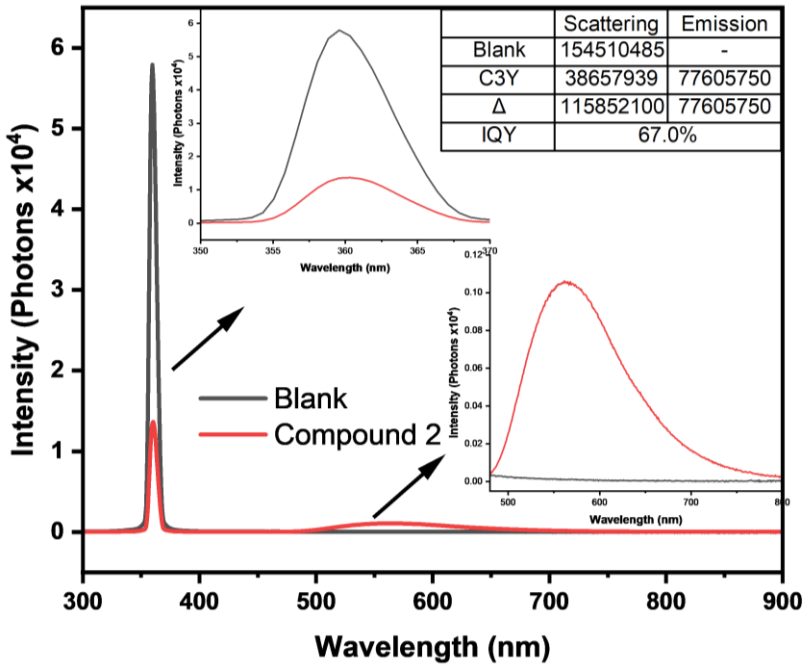


| | Scattering | Emission |
|---|---|---|
| Blank | 154510485 | - |
| C3Y | 38657939 | 77605750 |
| Δ | 115852100 | 77605750 |
| IQY | 67.0% | |

**Figure S11**. Details of PLQY measurement of compound **2.**

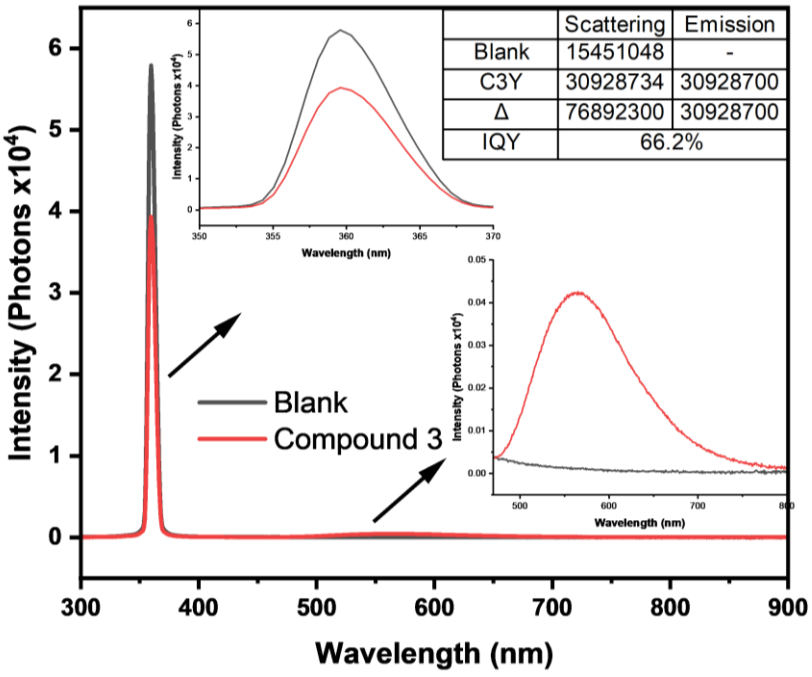


| | Scattering | Emission |
|---|---|---|
| Blank | 15451048 | - |
| C3Y | 30928734 | 30928700 |
| Δ | 76892300 | 30928700 |
| IQY | 66.2% | |

**Figure S12**. Details of PLQY measurement of compound **3.**

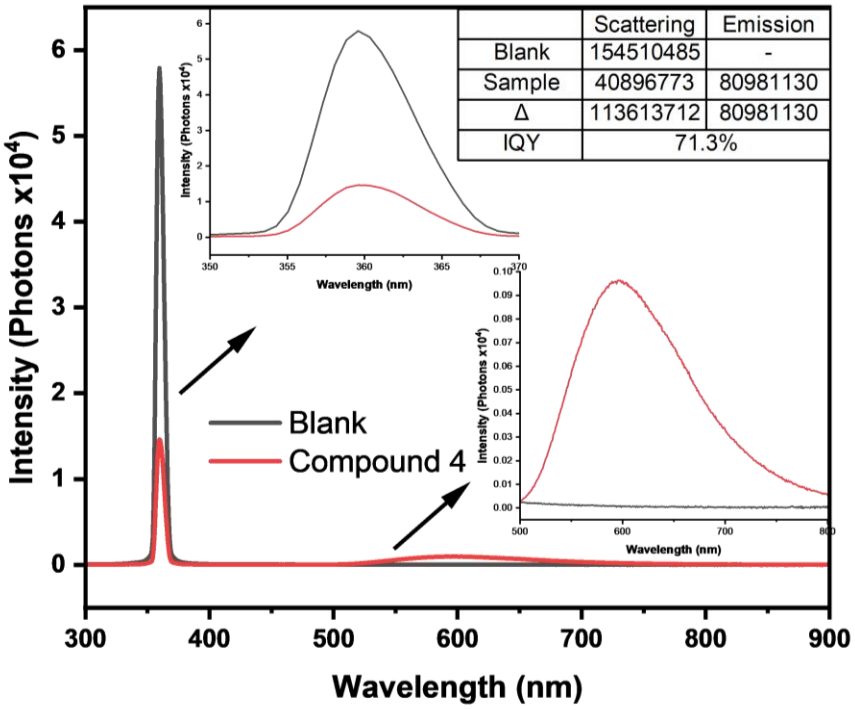


| | Scattering | Emission |
|---|---|---|
| Blank | 154510485 | - |
| Sample | 40896773 | 80981130 |
| Δ | 113613712 | 80981130 |
| IQY | 71.3% | |

**Figure S13**. Details of PLQY measurement of compound **1.**

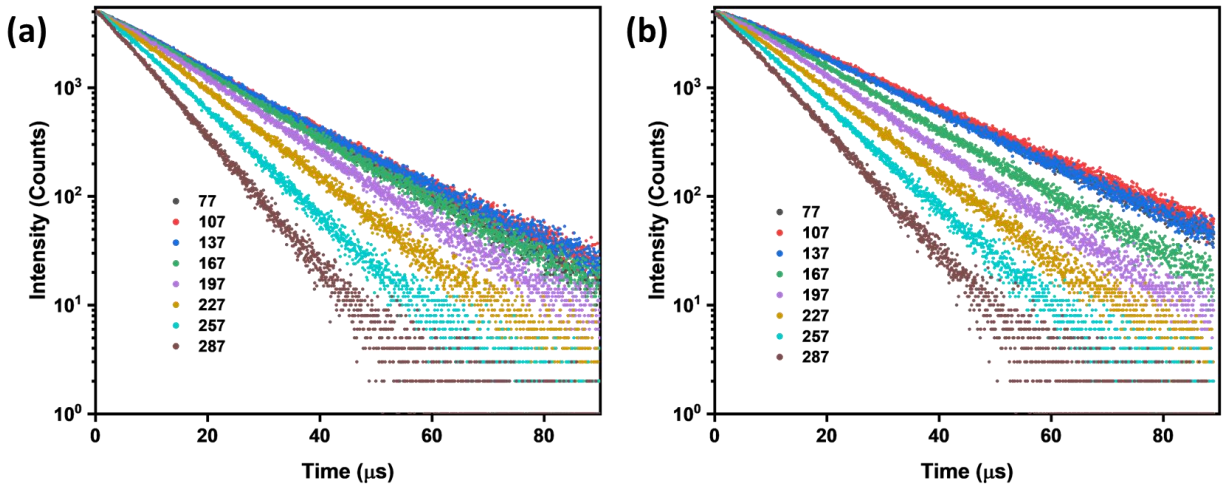


**Figure S14**. Luminescence decay curves of compounds (a) **3** and (b) **4** at various temperatures.

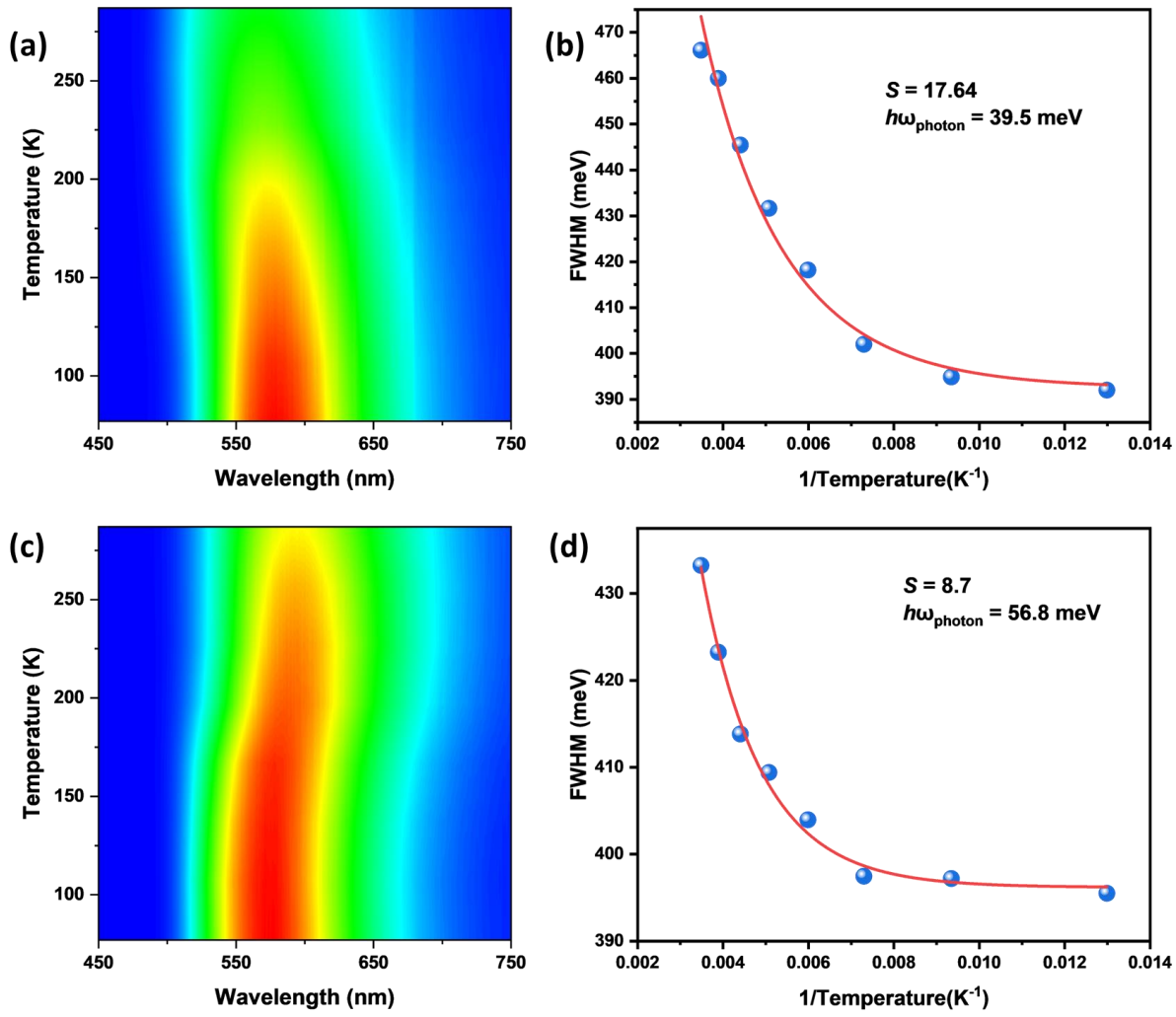


**Figure S15**. Temperature-dependent PL spectra of compounds (a) **3** and (c) **4**. Huang–Rhys factor (*S*) and photon frequency ($\hbar\omega_{photon}$) fitting curves of compounds (b) **3** and (d) **4**.

**Table S2.** Lifetime values of all compounds at various temperatures.

| Temperature (K) | Lifetimes (μs) | | | |
|---|---|---|---|---|
| | **Compound 1** | **Compound 2** | **Compound 3** | **Compound 4** |
| **77** | 20.1 | 25.2 | 15.5 | 18.9 |
| **107** | 20.1 | 24.9 | 16.1 | 19.2 |
| **137** | 19.9 | 22.5 | 15.9 | 17.3 |
| **167** | 18.4 | 19.3 | 14.9 | 15.2 |
| **197** | 16.1 | 16.4 | 13.3 | 13.1 |
| **227** | 13.2 | 12.6 | 11.2 | 11.1 |
| **257** | 10.3 | 10.4 | 9.1 | 9.2 |
| **287** | 8.2 | 8.4 | 7.1 | 7.6 |
| **RT** | 6.1 | 6.5 | 5.1 | 6.5 |

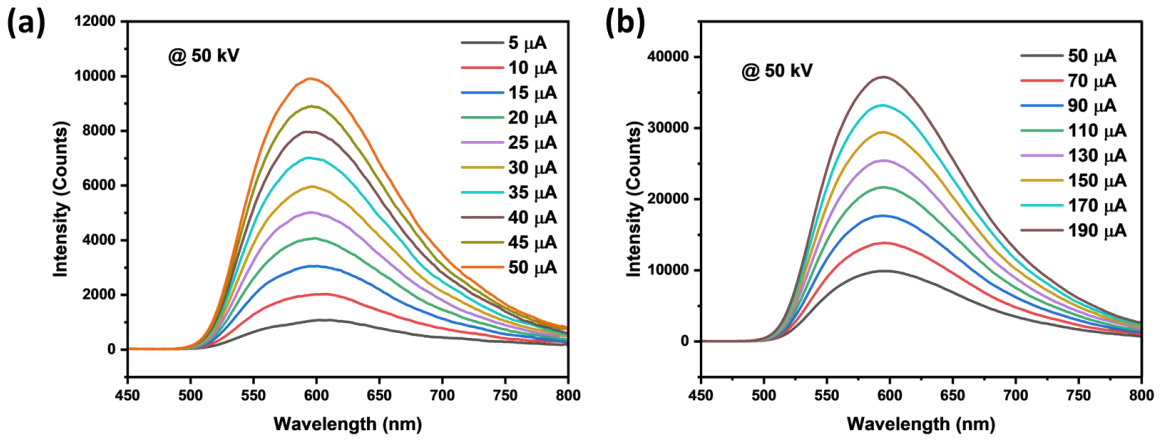


**Figure S16**. Current-dependent RL spectra of compound **1** at 50 kV.

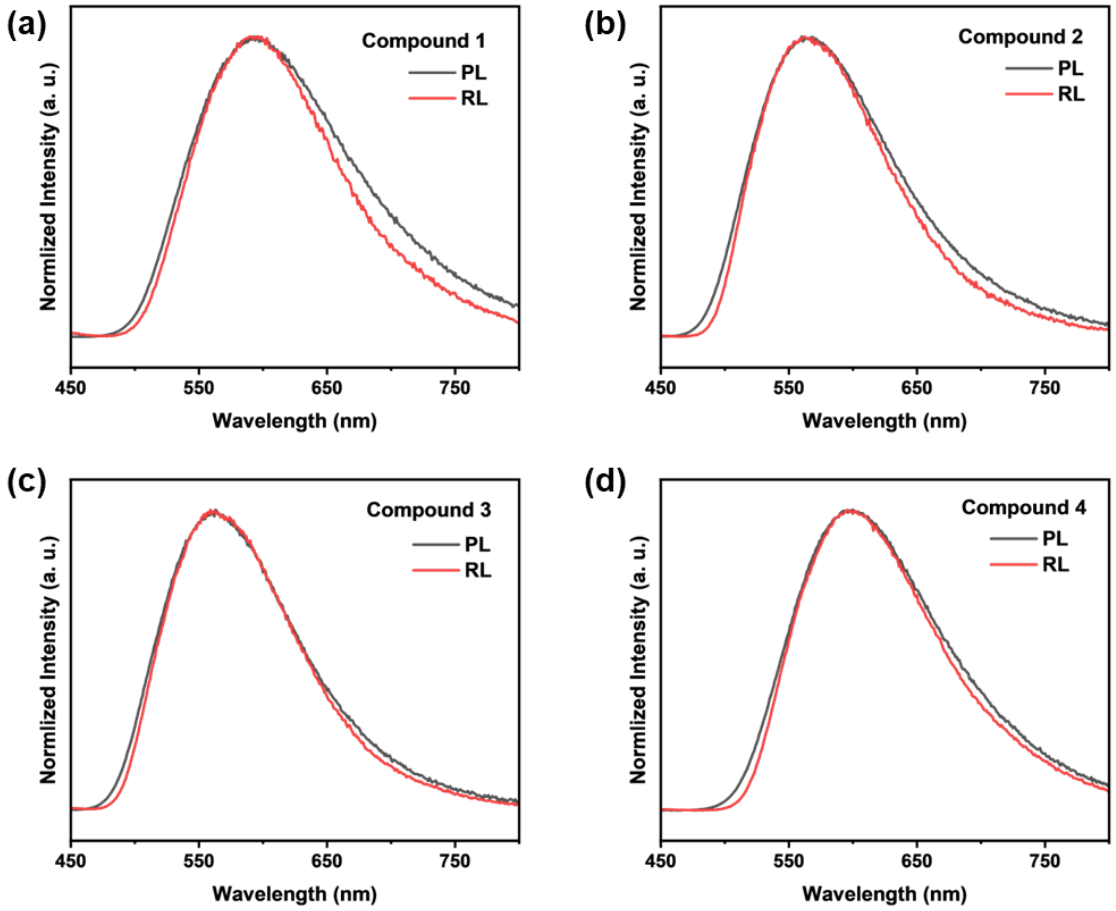


**Figure S17**. The RL and PL comparison of compounds (a) **1**, (b) **2**, (c) **3**, and (d) **4**.

# S6. References

(1) Hei, X.; Teat, S. J.; Liu, W.; Li, J. Eco-friendly, solution-processable and efficient low-energy lighting phosphors: copper halide based hybrid semiconductors Cu4X6(L)2 (X = Br, I) composed of covalent, ionic and coordinate bonds. *Journal of Materials Chemistry C* **2020**, *8* (47), 16790-16797, 10.1039/D0TC04672H. DOI: 10.1039/D0TC04672H.
(2) Hei, X.; Liu, W.; Zhu, K.; Teat, S. J.; Jensen, S.; Li, M.; O'Carroll, D. M.; Wei, K.; Tan, K.; Cotlet, M.; et al. Blending Ionic and Coordinate Bonds in Hybrid Semiconductor Materials: A General Approach toward Robust and Solution-Processable Covalent/Coordinate Network Structures. *Journal of the American Chemical Society* **2020**, *142* (9), 4242-4253. DOI: 10.1021/jacs.9b13772.
(3) Chen, X.; Song, J.; Chen, X.; Yang, H. X-ray-activated nanosystems for theranostic applications. *Chemical Society Reviews* **2019**, *48* (11), 3073-3101, 10.1039/C8CS00921J. DOI: 10.1039/C8CS00921J.
(4) Yanagida, T. Inorganic scintillating materials and scintillation detectors. *Proceedings of the Japan Academy, Series B* **2018**, *94* (2), 75-97. DOI: 10.2183/pjab.94.007.
(5) Robinson, K.; Gibbs, G. V.; Ribbe, P. H. Quadratic Elongation: A Quantitative Measure of Distortion in Coordination Polyhedra. *Science* **1971**, *172* (3983), 567-570. DOI: 10.1126/science.172.3983.567 (acccessed 2024/07/28).